[1] **Moulay Fatima**
[2] **Habbatti Assia**

Performances of an Asynchronous Motor Powered by a Photovoltaic Generator

Journal of Electrical Systems

Abstract: - One of the most exploited renewable energies in the world is photovoltaic solar energy. The objective of this work is the evaluation of the performance of a photovoltaic generator in different climatic conditions (temperature and irradiation) and when connected to an induction motor.

This photovoltaic system includes a DC-DC converter controlled by MPPT (disturbance and observation) control and a two-level inverter controlled by PWM technique.

Firstly, we studied the effect of the variation in irradiation and temperature on the operation of the photovoltaic module; secondly, we addressed the robustness and reliability of the boost converter and the MPPT control as well as the simplicity of the P&O method and the sine triangle. PWM control used for inverter. Finally, the contribution of the flow control method oriented towards stabilizing the speed of the asynchronous motor during the application of the load. Designed in MATLAB/Simulink, the system studied is more robust and more efficient and according to the satisfactory results, we can suggest the effectiveness and use of this model.

Keywords: Modelling, PV system, duty pulses generator, MPPT (P&O), Induction motor, Boost Converter, PWM.

I. INTRODUCTION

Since the generalization of the use of electricity, the world energy consumption is in very strong growth in all the regions of the world. Consumption will continue to increase either in electrical or economic terms.[1],[2]. Renewable energies (wind, sun, biomass, etc.) are all natural and unlimited resources that can be used to generate electrical energy.[3] Today, the sun is an inexhaustible and clean energy source, it could cover several thousand times compared to other global energy resources. The objective of our work is the study and simulation of a photovoltaic system. This system is composed of a GPV photovoltaic generator, and a DC/DC converter controlled by a pulse generator and which can be controlled by MPPT. The latter supplies an asynchronous machine from an inverter controlled by the PWM sine-delta type control.

Our work is based on an autonomous PV system without battery in order to see the performance of a PV generator supplying an asynchronous motor in variable climatic conditions on one side. On the other side, the impact of these variations on the asynchronous motor. The latter can itself supply another load, such as a pump (PV pumping), a conveyor, etc.

The paper is structured as follows, first we represent a generality on the photovoltaic system by giving an overview of the PV effect and the cell which is the heart of the solar panel in order to define the field and the photovoltaic generator [4].

In the second part, we detail the modeling of the photovoltaic system, starting with the modeling of each element. For the DC/DC converter, we chose the Boost chopper [5]. A classic two-level inverter controlled by the sine-delta type PWM control is used, the purpose of which is to synchronize its output power with that injected into the asynchronous motor. The last, the work is intended for the simulation of the photovoltaic system. Each element was simulated separately in order to evaluate their performance before simulating the entire SPV photovoltaic system. Finally, our work is closed by a general conclusion through which, we exposed the main results that we obtained. The set of tests carried out on the studied system were developed under the Simulink / Matlab environment.

[1] Faculty of Techology, Smart Grids & Renewable Energies (S.G.R.E) Laboratory Djillali Liabès University, Sidi Bel Abbés. Algeria.
Email: fatimamoulay66@yahoo.fr;
[2] Faculty of Techology, Smart Grids & Renewable Energies (S.G.R.E) Laboratory University Bechar, Algeria.
Email: bellia_abdeljalil@yahoo.fr

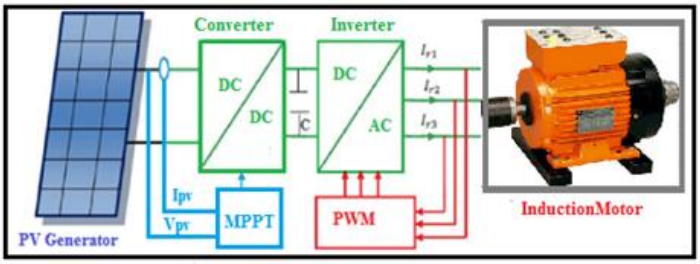

Fig. 1 Synoptic diagram of the PV system

II. The Photovoltaic System

The PV photovoltaic system consists of an energy source (photovoltaic generator), a power interface (the static DC-DC and DC-AC converters with a control system) and a load. The main role of the static converter is to make an impedance match so that the generator delivers the maximum energy [6].

Photovoltaic solar energy is a form of renewable energy that produces electricity by transforming solar radiation through a photovoltaic cell. Several cells are connected together and form a photovoltaic solar panel (or module). These are grouped together and are called photovoltaic field.

Side of The photovoltaic cell is made of a semiconductor material that absorbs light energy and transforms it directly into electric current. The conversion of solar energy into electrical energy is based on the photovoltaic effect, i.e. on the ability of photons to create charge carriers (electrons and holes) in a material[7].

When a semiconductor is illuminated with radiation of the appropriate wavelength, the energy of the absorbed photons allows electronic transitions from the valence band to the conduction band of the semiconductor, thus generating electron-hole pairs , which can contribute to the current transport by the material when it is polarized [8].

A. Photovoltaic module (panel)

To produce more power, the cells are assembled to form a module. A series association of several cells gives a solar module (also called photovoltaic panel), and a series and/or parallel association of several modules makes it possible to create a photovoltaic field [9].

A photovoltaic module generally consists of a circuit of 36 cells in series, protected from humidity by a glass and plastic encapsulation. The assembly is then fitted with a frame and an electrical junction box [10].

Modules grouped in series will increase the voltage. On the other hand, those grouped in parallel will deliver a greater current. The grouping of the modules gives a photovoltaic panel.

B. GPV photovoltaic generator

A photovoltaic generator is a complete system (set of equipment in place) ensuring the production and management of the electricity supplied by the photovoltaic sensors.

The energy is used immediately, injected into the electrical network or stored in accumulators depending on the type of application.

III. Modeling Of The Photovoltaic System

Our system is composed of a GPV, a step-up chopper (Boost), an inverter and an asynchronous motor. This part of the work is intended for the modeling of the PV photovoltaic system by giving an illustration on each element. We will present the mathematical model of a cell and a GPV, the DC-DC converter and their different types, then we will model the Boost chopper, the DC-AC converter (the inverter). Thus the principle of the PWM control by specifying that of sinus-triangle.

A. Modeling of PV cells

PV cells are connected together to form photovoltaic module or photovoltaic panel [5]. The equivalent circuit of a solar cell is shown in Fig. 2. There are mathematical models of the characteristic current–voltage of the photovoltaic cell. However, the most practical by their relative simplicity in the calculation are the single exponential model (a single diode), in which, the obscurity current (diode current), representing uniquely the saturation current resulting of the diffusion phenomenon and the two-exponential model (two diodes) representing both the components, diffusion and recombination [11].

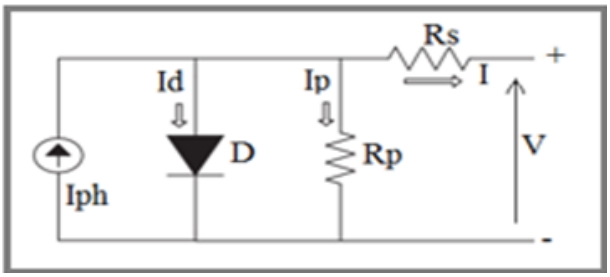

Fig. 2 Equivalent circuit of the photovoltaic module

The equivalent circuit of the chosen photovoltaic module is the one-exponential (one-diode) model in which the dark current (diode current), representing only the saturation current resulting from the diffusion phenomenon (fig.3). Saturation and the mechanical power *Pm* available on the shaft of the electric generator are given by equations (1) and (2) [7]:

$$I = I_{ph} - I_0\left[\exp\left(\frac{e(V+R_sI}{\lambda KT_c}\right)-1\right]-\frac{V+R_sI}{R_p} \quad (1)$$

$$P_m = \frac{1}{2}C_p\left((\Omega_2\cdot R)/(K\cdot V_v)\right)p\pi\cdot R^2\cdot V_v^{\ 3} \quad (2)$$

V: The voltage at the terminals of the module,
λ :Coefficient characterizing the power variation as a function of temperature,
K: Boltzmann constant,
e :Charge of the electron,
I_0 : Saturation current
T: Cell working temperature
R_s and R_p Resistors represent the losses of metal contacts and leakage of the PN junction respectively.

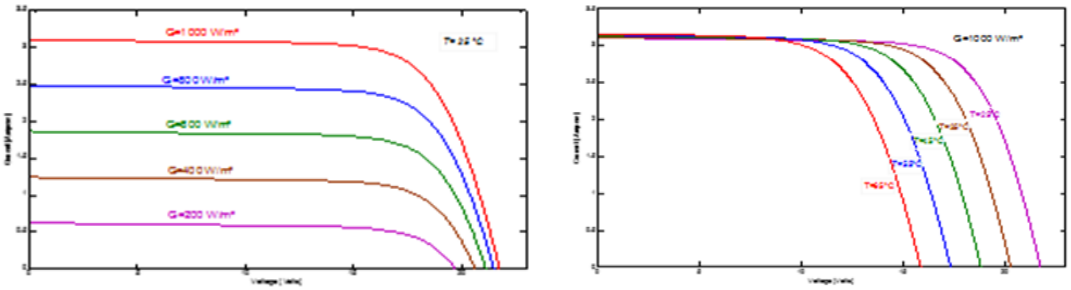

Fig.3 I(V) by varying the irradiance and I(V) by varying the temperature

Increasing irradiance results in a large increase in short circuit current but a slight increase in open circuit voltage. High temperature lowers the open circuit voltage for fixed radiation.
PWX 500 PV module (49W) characteristics at 25°C and 1000W/m^2.

Table I. Parameters of the PV Module

Parameters	Values
P max	49 W
Imp	2.88 A
Vmp	17 V
Isc	3.11 A
Voc	21.8 V
RS	0.45 Ω
RP	310 Ω
Ns	36

B. Boost converter (parallel chopper):

The chopper is a DC/DC converter that converts DC energy at a given voltage (or current) level into DC energy at another voltage (or current) level [12].

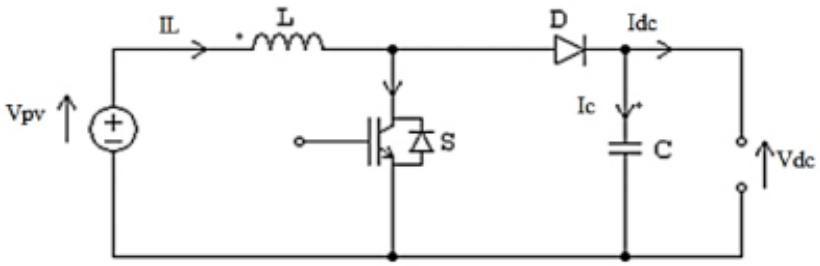

Fig. 4 Electrical circuit of the Boost converter.

The PV voltage at MPP, Vpv = 100 V appears as the input voltage source (Vs) while DC link voltage of VSI, Vdc=380V appears as output voltage of boost converter.

The duty cycle, D of the boost converter is estimated to be :

Duty Cycle (D)

$$D = \frac{V_{dc} - V_{pv}}{V_{dc}} = \frac{380 - 100}{380} = 0.736 \tag{3}$$

Value of Inductor (L)

Calculate minimum inductance

$$L_{\min} = \frac{(1-D)R}{2 * f} \tag{4}$$

Calculate 25% larger than minimum inductance

$$L = 1.25 * L_{\min} \tag{5}$$

Calculate minimum capacitance

$$C = \frac{1-D}{8L(0.05)f^2} \tag{6}$$

Table 2. Specification of Boost Converter

Parameters	Values
Input Voltage, (Vpv)	100V
Output Voltage, (Vdc)	380V
Duty Cycle, (D)	0.736
Ripple Voltage, (Vripple)	1% of Vo
R load	50 Ω
switching frequency	1kHz
Ripple Current, (Iripple)	10% of Io
Inductor, (L)	4.5mH
Capacitor, (C)	2640µF

C. Control of the DC/DC converter by the MPPT method

There are many methods for controlling the power delivered by the photovoltaic generator which can be classified according to different criteria [13].

But they all remain dependent on measurements of the voltage and current of the PV generator. We can, however, cite those that are most often encountered in the literature and which are used in this work [14].

The P&O disturbance and observation method.

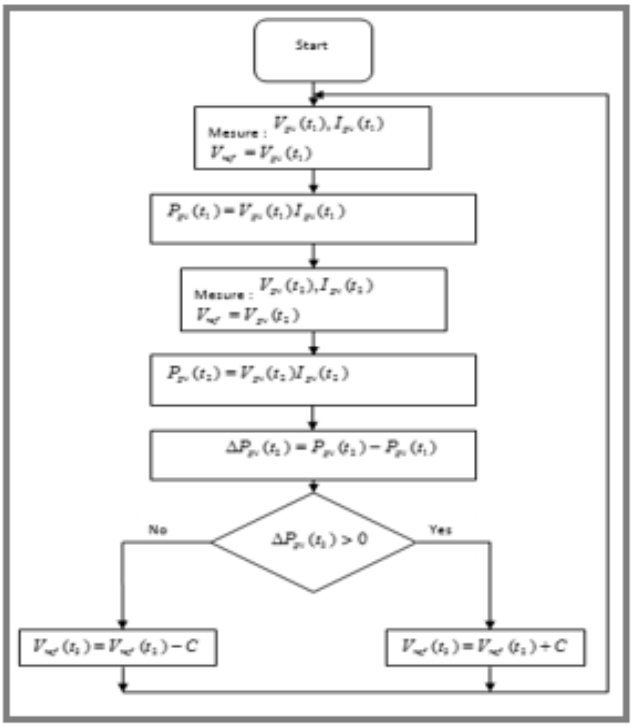

Fig. 5 The P&O disturbance and observation method

This is the method most used in practice. It is an iterative method for obtaining the maximum PPM power point. It consists of tracing the characteristic of the PV field: P (V), then creating a disturbance and observing the direction of the change, as shown in the algorithm in fig. 4.

D. DC/AC converter

1). Modeling of the voltage inverter and its control

It is assumed that all the elements constituting the circuit of the power supply system are perfect [15].

The main circuit of the power supply system represented by fig. 6 has, on the network side, a supposedly perfect diode rectifier bridge, it is followed by a passive filter LC, that has an inductance L and a capacitance C, whose main role is to reduce current and rectified voltage ripples [16].

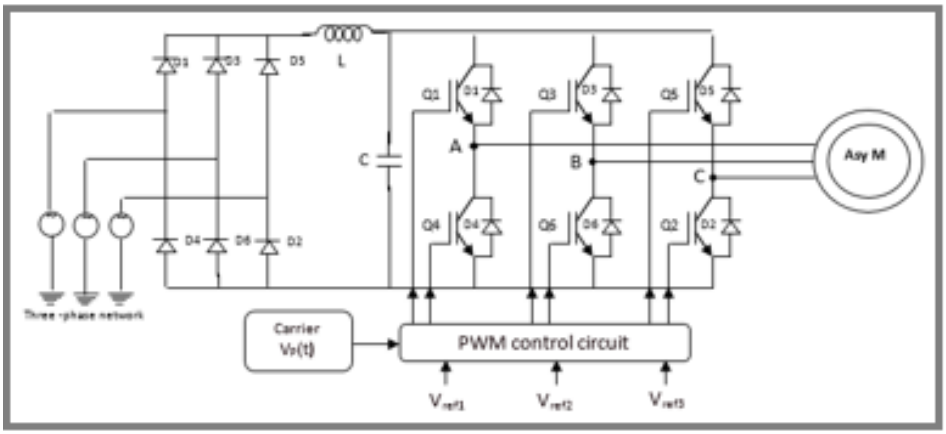

Fig. 6 General structure of the power supply system

The inverter makes it possible to generate a modulated voltage, from a DC voltage, the amplitude and frequency of which are variable [17].

2). Mathematical model of the three-phase inverter

We can replace each transistor-diode group of fig. 6 by switches kj, k'j with (j = 1, 2, 3), we obtain the simplified diagram as shown in fig. 7

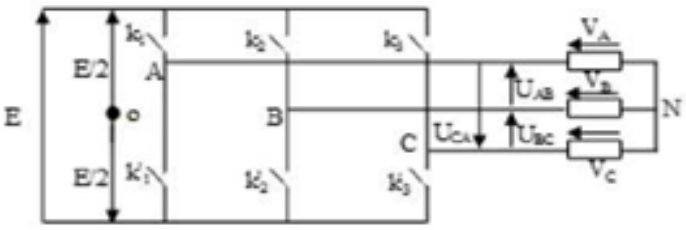

Fig. 7 Two-level three-phase voltage inverter

Pulse width modulation (PWM) control

In the form of Simulink blocks, the generation of pulses can be represented by the following diagram [18].

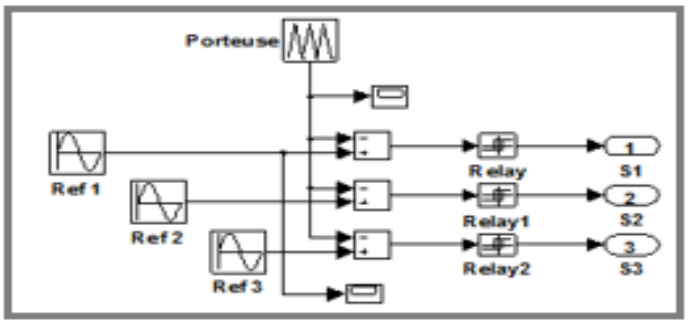

Fig.8 Block diagrams of the PWM technique under Simulink

E. Modelling of the Asynchronous Machine

Directly connected to the constant voltage and frequency industrial network, it rotates at a speed not very different from the synchronous speed; it is he who is used for the realization of almost all constant speed training. It also allows the realization of variable speed training and the place it occupies in this field continues to grow [19].

For a three-phase asynchronous machine supplied with voltage, the stator voltages $(V_{ds}\ V_{qs})$ and the speed of the rotating field are considered as control variables, the resistive torque Cr as disturbance. We choose in our case, the following state vector: $X_u^T = \left(I_{ds}\ I_{qs}\ \phi_{dr}\ \ \phi_{qr}\right)$.

This choice of variable is justified on the one hand by the fact that the stator currents are measurable and on the other hand by the desire to control the norm of the rotor flux in the control law [20].

After simplification and rearrangement of the equations of the asynchronous machine in the Park frame, we obtain the model of the machine in the form of an equation of state:

$$\dot{\mathbf{X}}_\mathbf{u} = \mathbf{A}_\mathbf{u}\mathbf{X}_\mathbf{u} + \mathbf{B}_\mathbf{u}\mathbf{U} \tag{7}$$

With:

$$A_u = \begin{bmatrix} -\lambda & \omega_s & \frac{K}{T_r} & \omega_r K \\ -\omega_s & -\lambda & -\omega_r K & \frac{K}{T_r} \\ \frac{L_m}{T_r} & 0 & -\frac{1}{T_r} & \omega_{sl} \\ 0 & \frac{L_m}{T_r} & -\omega_{sl} & -\frac{1}{T_r} \end{bmatrix}$$

$$B_u = \begin{bmatrix} \frac{1}{\sigma L_s} & 0 \\ 0 & \frac{1}{\sigma L_s} \\ 0 & 0 \\ 0 & 0 \end{bmatrix} U = \begin{bmatrix} V_{ds} \\ V_{qs} \end{bmatrix} \tag{8}$$

With:

$$T_r = \frac{L_r}{R_r}, K = \frac{L_m}{\sigma L_s L_r}, \sigma = 1 - \frac{L_m^{\ 2}}{L_r L_s}, \lambda = \frac{R_s}{\sigma}.\frac{1}{L_s} + \frac{L_m^{\ 2}}{\sigma}.\frac{R_r}{L_s.L_r^{\ 2}}$$

To these electrical equations, we must associate the mechanical equation to obtain the complete model of the system:

$$C_e = \frac{3}{2} p \frac{M}{L_r} (\phi_{dr} I_{qs} - \phi_{qr} I_{ds}) \tag{9}$$

$$\frac{d\Omega_r}{dt} = (C_e - C_r - f_r \Omega_r) / J \tag{10}$$

Then the model of the MAS supplied with voltage is found with 5 equations (2 magnetic + 2 electrical + 1 mechanical).

IV. Simulation Of A Pv-Boost Panel With Induction Motor

A. Block diagram with MPPT Control

The last fig. represents the grouping of the photovoltaic generator, the booster chopper with MPPT Control, the PWM inverter, and the induction motor.

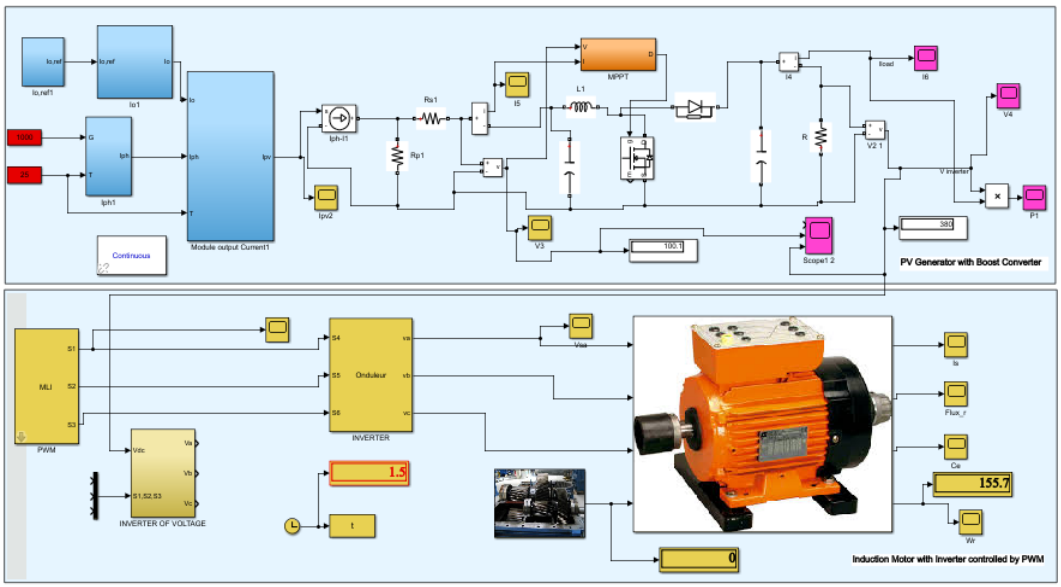

Fig. 9 The PV system simulation block powering a AC motor with MPPT (P&O) Control (Simulink / Matlab)

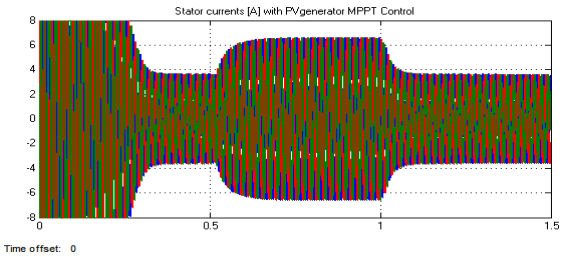

Fig. 10 The stator currents of the three phases (isa, isb and isc) as a function of time

The fig. 10, represents the 3 stator currents by applying a load of t=0.5 sec until t=1 sec, we notice a current draw (increase in amplitude) in this interval to meet the need.

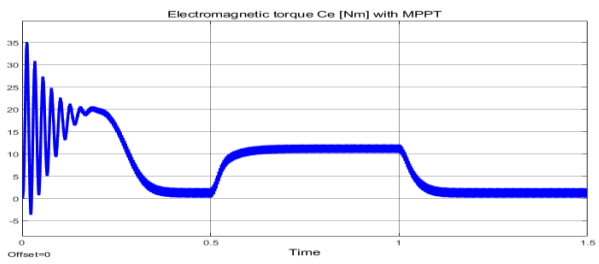

Fig. 11 The electromagnetic torque as a function of time

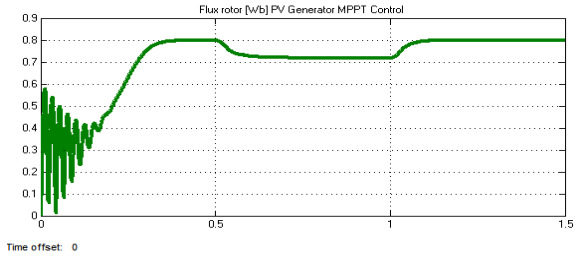

Fig. 12 The Rotor Flux as a function of time

The fig. 12, shows the natural coupling existing between the flux and the electromagnetic torque

The evolution of the torque in the time interval 0 and 1.5 sec is a typical characteristic rate of all induction motors. This presents very significant pulsations at the first moments. During the transient regime, the torque is strongly pulsating, then stabilizes at the end of the regime. The electromagnetic torque evolves and during the load regime, it responds to the current draw (fig. 11).

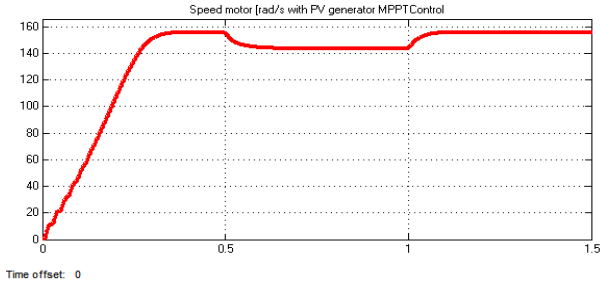

Fig. 13 The rotor speed as a function of time

For the appearance of the speed presented in the figure, we noticed that the rotation speed of the motor will evolve over time and reaches its nominal speed (156 rad/s) in a slow time, with a tendency to oscillate due to the inertia of the rotating masses and the damping coefficient due to the low values of the flows. And during the application of the load this speed decreases in the interval t=0.5 sec until t=1 sec (Fig. 13).

B. The field-oriented control (FOC)

The principle of field-oriented control is based on the control of both the magnitude and the angle of each phase current and voltage [15].

The torque control is normally achieved by controlling the armature with constant field current. The Field weakening is employed to increase the speed beyond a base speed. The simplicity and flexibility of control of DC motors have made them suitable for variable speed drive applications. In the field-oriented control, d-q coordinate's reference frame locked to the rotor flux vector used to achieve decoupling between the motor flux and torque. They can thus be separately controlled by stator direct-axis current and quadrature-axis current respectively, like in a DC motor [19].

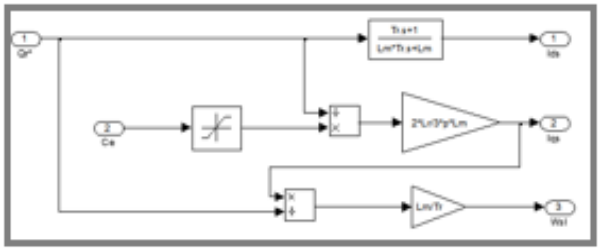

Fig. 14 Block diagram of the orientation of the rotor flux (OFR).

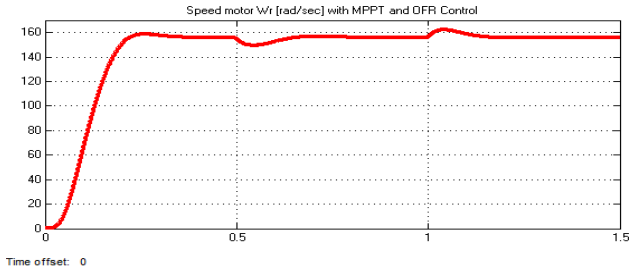

Fig. 15 The rotor speed as a function of time

For the motor speed, we note that despite the presence of the disturbance at t=0.5sec until t=1 sec, the speed remains unchanged and this shows the effectiveness of the speed control used, with field-oriented control (fig. 15).

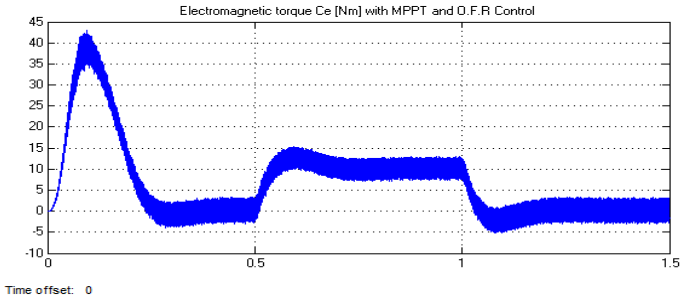

Fig. 16 The electromagnetic torque as a function of time

At the fig. 16, in the case of the application of oriented flow control, during the transient regime, the torque is less pulsating, comparing it to Fig. 11

V. Conclusion

The objective of the simulation is to see the influence of temperature and sunshine on the operation of the GPV and implicitly on its current-voltage characteristic. The conclusion we have reached is that the performance of the solar panel is dependent on temperature and irradiation. It has been noticed that the current increases when the temperature or the irradiation increase, while this generates a considerable decrease in the level of the voltage and implicitly on the energy efficiency of the panel and the GPV. On the other hand, the increase in the irradiation generates an increase in the level of the current and the power, but it does not influence much on the tension.

In order to permanently extract the maximum power available at the generator terminals and generate it to the induction motor, a Boost chopper has been associated and must be controlled by a maximum power point tracking algorithm. In our study, a two-level inverter was used to convert DC voltage to AC voltage. It also plays the role of source-load adapter when controlled by the PWM technique. It was concluded that the presence of power electronics is essential in the photovoltaic system in order to adapt and ensure its proper functioning. The inverter generally generates harmonics which can disturb the system. Therefore, filtering between the inverter and the load is necessary in order to minimize the non-sinusoidal signals generated by the inverter.

The simulation results obtained showed the natural coupling existing between the flux and the electromagnetic torque, and the transient regime of the induction machine is improved by applying the oriented flux method.

References

[1] Le An and D.D.-C. Lu, “Design of a Single-Switch DC/DC Converter for a PV-Battery-Powered Pump System With PFM+PWM Control,” IEEE Transactions on Industrial Electronics, vol. 62, no. 2, pp. 910 - 921, Feb. 2015..

[2] Loukriz, D. Saigaa, M. Drif, M. Hadjab, M H Moufdi, A. Houari, S. Messalt, M.A. Saeed. (2021) A New Simplified Algorithm for Real-Time Power Optimization of TCT Interconnected PVArray under Any Mismatch Conditions. Journal Européen des Systèmes Automatisés, Vol. 54, No. 6, pp. 805-817. https://doi.org/10.18280/jesa.540602.

[3] El Halim, A.A.E.B., Bayoumi, E.H.E. (2021). Using a new combination of P&O and ICM methods for the experimental validation of MPPT efficacy. Journal Européen des Systèmes Automatisés, Vol. 54, No. 6, pp. 797-804. https://doi.org/10.18280/jesa.540601.

[4] G. Lorenzini, M.A. Kamarposhti, A.A.A. Solyman, (2021). Maximum power point tracking in the photovoltaic module using incremental conductance algorithm with variable step length. Journal Européen des Systèmes Automatisés, Vol. 54, No. 3, pp. 395-402. https://doi.org/10.18280/jesa.540302

[5] Saeed, M.A.; Kim, S.H.; Kim, H.; Liang, J.; Woo, H.Y.; Kim, T.G.; Yan, H.; Shim, J.W. Indoor Organic Photovoltaics: Optimal CellDesign Principles with Synergistic Parasitic Resistance and Optical Modulation Effect. Adv. Energy Mater. 2021, 11, 2003103.]

[6] H. Taghvaee, M. A. M. Radzi, S. M. Moosavain, Hashim Hizam and M. Hamiruce Marhaban, “A Current and Future Study on Non-isolated DC–DC Converters for Photovoltaic Applications,” Renewable and Sustainable Energy Reviews, vol. 17, pp. 216-227, Jan. 2013.

[7] Errouha, M.; Derouich, A.; Motahir, S.; Zamzoum, O. Optimal Control of Induction Motor for Photovoltaic Water Pumping System. Technol. Econ. Smart Grids Sustain. Energy 2020, 5, 6.

[8] S.Tyagi, GVerma, « Simulation et analyse du convertisseur DC-DC Boost à l'aide d'un contrôleur de mode coulissant dans des conditions variables», (IOSR-JEEE), Volume 13, Issue 1 Ver. II (Jan.2018)

[9] Motahhir, S.; El Hammoumi, A.; El Ghzizal, A. The Most Used MPPT Algorithms: Review and the Suitable Low-cost Embedded Board for Each Algorithm. J. Clean Prod. 2019, 246, 118983.

[10] Q. Al-Shetwi, M. Z. Sujod, A. Al Tarabsheh, and I. A. Altawil. 2016. Design and Economic Evaluation of Electrification of Small Villages in Rural Area in Yemen Using Stand-Alone PV System. International Journal of Renewable Energy Research (IJRER), vol.6. No. 1. pp. 290-298.
[11] J. Liang et al. "Evolutionary multi-task optimization for parameters extraction of photovoltaic models," Energy Convers. Manag., Vol. 207, p. 112509, 2020
[12] F. A. Hashim, E. H. Houssein, K. Hussain, M. S. Mabrouk, and W. AlAtabany, "Honey Badger Algorithm: New metaheuristic algorithm for solving optimization problems," Math. Comput. Simul., Vol. 192, pp. 84-110, 2022
[13] Y. Agrebi, Y. Koubaa and M. Boussak "Online Rotor ResistanceEstimation Using the Model Reference Adaptive System of Induction Motor", i-manager's Journal of Electrical Engineering, vol. 3 no 3 January- March 2010.
[14] Y. Xing, "A novel rotor resistance identification method for an indirect rotor flux-oriented controlled induction machine system,". IEEE Trans. Power Electron., vol. 17, pp. 353–364, 2002
[15] S. Jain, A.K. Thopukara, R. Karampuri and V.T. Somasekhar, "ASingle-Stage Photovoltaic System for a Dual-Inverter-Fed Open-End Winding Induction Motor Drive for Pumping Applications," IEEE Transactions on Power Electronics, vol. 30, no. 9, pp. 4809 - 4818, Sept. 2015.
[16] Singh and V. Bist, "A BL-CSC Converter-Fed BLDC Motor Drive with Power Factor Correction," IEEE Transactions on Industrial Electronics, vol. 62, no. 1, pp. 172-183, Jan. 2015.
[17] T.J.Liang and L.S.Yang , Analysis and implementation of a novel bidirectional dc–dc converter,‖ IEEE Trans. Industrial Electron., vol. 59, no. 1, pp. 422–434, Jan. 2012.
[18] Tsorng -Ju Liang, Shih-Ming Chen, Lung-Sheng Yang, and JiannFuh Chen, A safety enhanced high step up DC-DC converter for ACPhotovoltaic module application‖ IEEE Transaction. On Power Electron., vol.27, no.4.,April 2012
[19] Wang, F.; Zhang, Z.; Mei, X.; Rodríguez, J.; Kennel, R. Advanced control strategies of induction machine: Field oriented control, direct torque control and model predictive control. Energies 2018, 11, 120
[20] Ehsan Hosseini, « Modélisation et simulation de commutation de hacheurs via matlab/Simulink »,Bulletin Scientifique du Petru Maior, Université de Tîrgu Mures, Vol. 12, 2015.

APPENDIX

Asynchronous Machine Parameters

Power: P=1.5kw;
Voltage: U=380/220V;
Frequency: f=50Hz;
Rotation speed: N=1450rpm;
Number of pole pairs: p=2;
Stator resistance: Rs=4.85Ω;
Rotor resistance: Rr=3.81Ω;
Stator inductance: Ls=0.274H;
Rotor inductance: Lr=0.274H;
Mutual inductance: Lm=0.258H;
The moment of inertia: J=0.031kg.m2;
The coefficient of friction: fr=0.0114N.m/rd/s.